Anal Bioanal Chem (2010) 398:3015–3021
DOI 10.1007/s00216-010-4253-z

ORIGINAL PAPER

Biosilicated CdSe/ZnS quantum dots as photoluminescent transducers for acetylcholinesterase-based biosensors

Raluca Buiculescu · Maria Hatzimarinaki · Nikos A. Chaniotakis

Received: 10 August 2010 / Revised: 20 September 2010 / Accepted: 23 September 2010 / Published online: 9 October 2010

Abstract CdSe/ZnS core/shell quantum dots (QDs) are functionalized with mercaptoundecanoic acid (MUA) and subsequently covered with poly-L-lysine (PLL) as the template for the formation of the silica outer shell. This nanocomposite is used as a transduction and stabilization system for optical biosensor development. The covalent immobilization of the enzyme acetylcholinesterase from *Drosophila melanogaster* (AChE) during the formation of the biomimetically synthesized silica is used here as a model, relatively unstable enzyme, as a proof of principle. The enzyme is successfully immobilized onto the QDs and then stabilized by the PLL capping and the subsequent formation of the outer nanoporous silica thin shell, giving rise to the QD/AChE/PLL/silica biosensor. It is shown that the poly-L-lysine templated silica outer shell does not modify the optical properties of the quantum dots, while it protects the enzyme from unfolding and denaturation. The small pores of the silica shell allow for the free diffusion of the analyte to the active center of the enzyme, while it does not allow for the proteases to reach the enzyme. The response of the QD/AChE/PLL/silica nano-biosensor to its substrate, acetylcholine chloride, is evaluated by monitoring the changes in the QDs' photoluminescence which are related to the changes in pH. These pH changes of the surrounding environment of the QDs are induced by the enzymatic reaction, and are associated with the analyte concentration in the solution. The biodetection system proposed is shown to be stable with a storage lifetime of more than 2 months. The data presented provides the grounds for the application of this nanostructured biosensor for the detection of AChE inhibitors.

Keywords Quantum dots · Acetylcholinesterase (AChE) · Biomimetically synthesized silica · Photoluminescence · Nano-biosensor

R. Buiculescu · M. Hatzimarinaki · N. A. Chaniotakis (✉)
Laboratory of Analytical Chemistry, Department of Chemistry,
University of Crete Voutes,
P.O. Box 2208, 71003 Iraklion, Crete, Greece
e-mail: nchan@chemistry.uoc.gr
Url: www.analytical_chemistry.uoc.gr

Introduction

The investigation of processes involving a biological structure or molecule requires that these analytes are labeled with a marker whose signal can be easily observed via a facile transduction mechanism. Organic dyes have been intensively used in past years as photoluminescent tags and thus transducers for the detection of molecules involved in bio-medical processes. However, these organic fluorophores present a number of drawbacks, such as sensitivity to their local environment [1], fast photobleaching [2], fluorescence blinking [3], and relatively broad emission spectra [4].

Recently, semiconductor quantum dots have been used as alternative fluorophores in a variety of applications. Their small size and large surface-to-volume ratio [5], high photoluminescence quantum yields [6], narrow, symmetric, and size-tunable emission spectra covering the region from blue to red, photochemical stability as well as their sensitivity to the surrounding environment [7] make them ideal probes for biological labeling and sensing. After the pioneering work of Chan and Nie [8] which reported that semiconductor quantum dots could be used as an alternative to organic fluorophores for the labeling of transferrin and IgG, a great number of publications have followed. Quantum dots (QDs) have been used as donors/acceptors in FRET processes [9–12], for fluorescent imaging of living

cells [13], for the construction of pH sensors in solution [14, 15] or enzyme biosensors [16, 17]. They have also been conjugated to antibodies [18], cellular proteins [19], or receptors [20]. However, besides their advantages, some of the semiconductor QDs have the downside of being toxic, and thus less favorable for bio-applications [21]. This may be due to photochemical processes resulting in the irradiation of QDs under the aqueous aerobic conditions of in vitro cell imaging [22], the process having as result the release of toxic free Cd^{2+} ions. However, in a recently published study [23], Graf and co-workers report on a three- to four-times-lower release of toxic Cd^{2+} ions from CdSe/ZnS QDs doped silica colloids than those released from CdSe/ZnS QDs simply stabilized by organic ligands or biomolecules, result which indicates that coating the quantum dots delays this process and thus renders them suitable markers for in vivo studies. In a paper published 3 years before the study of Graf and co-workers, silica-coated QDs showed no cytotoxic effects in cell lines investigated with concentration as high as 30 μM [24]. These results prove that entrapment of the semiconductor QDs within silica provides the necessary protection from chemical degradation, reduce the degree of leaching of the toxic core material [25] and also present the advantages of hydrophilicity, biocompatibility, optical transparency, and chemical stability.

In particular, QDs coated with silica shells have been widely investigated. Up until now, many methods have been reported to coat QDs with a silica shell through Stöber-based approaches [26, 27], by reverse (water in oil) microemulsion method [28–31], or by promoting silicification by enzymes, such as silicatein [32], or polysaccharides, such as chitosan [33]. Some groups have reported on immobilizing proteins onto silica-coated quantum dots [34, 35] the obtained complex being suitable for use in biolabeling and imaging. Of special interest are the experiments performed for encapsulating enzymes within a silica matrix. Sol–gel is a widely used method for immobilization of enzymes [36–38] but due to harsh processing conditions that result in a loss of enzyme activity, new, milder methods of silicification, namely biosilicification, that use more biologically compatible reaction conditions, have been studied [39]. By using this method, the complete entrapment of the enzymes within the silica matrix has been confirmed, while, at the same time, managing to retain almost all of the initial activity of the enzyme. Recently, our group has studied the biosilicification of carbon nanofibers-immobilized enzymes, using a poly-L-lysine (PLL) templated silica matrix [40, 41], proving that this approach is suitable for stabilizing enzymes and protect them from denaturation factors.

In the present work, QD/acetylcholinesterase (AChE) conjugates have been entrapped for the first time into a PLL-templated silica matrix. CdSe/ZnS quantum dots have been chosen as a signal transducer due to their excellent photoluminescence efficiency and stability while they are also used for the covalent immobilization of AChE. Poly-L-lysine is a positively charged homo-polypeptide which interacts electrostatically to DNA, red cell membrane and any negatively charged protein. In this case, it provides the template for the formation of biomimetically synthesized silica [42]. The pores of the poly-L-lysine templated silica matrix allow the transport of the substrate to the entrapped QD/AChE conjugates and its subsequent conversion to products. The conjugation to the QDs and the entrapment inside the stable silica matrix is believed to increase the stability of the relatively unstable acetylcholinesterase from *Drosophila melanogaster*, protecting it from unfolding, denaturation, and attack from proteases [40]. Also, the poly-L-lysine templated silica matrix is expected to protect the QDs from chemical degradation and leaching of the toxic core materials [23–25, 43]. The detection system developed is shown to be stable, as it retains a big percentage of its activity after 2 months. While the quantum dots provide a sensitive optical transduction for the monitoring of the enzymatic reaction, the nanostructures offer a stabilization platform to the AChE-based detection system.

Materials and methods

Reagents

CdSe/ZnS core/shell nanocrystals (7.83×10^{-6} mol/L, dark red, mercaptoundecanoic acid coated) were purchased from NN-Labs (USA). Acetylcholinesterase from *D. melanogaster* (*Dm.* AChE, stock solution 8.338 U/mL) was kindly provided by Prof. Didier Fournier ("Paul Sabatier" University, Toulouse, France). Poly-L-lysine hydrobromide (PLL, MW 20,000–30,000) was obtained from Fluka. (2-[*N*-Morpholino]ethanesulfonic acid) hydrate (MES), *N*-ethyl-*N*′-(3-dimethylaminopropyl) carbodiimide (EDC), *N*-hydroxysulfosuccinimide sodium salt (NHS), tetramethyl orthosilicate (TMOS 99+%), and acetylcholine chloride were obtained from Sigma-Aldrich. In all experiments, nanopure water (~18 MΩ-cm, EASY pure model D7033, Barnstead) was used. All other reagents used were of analytical grade.

Preparation of QD/AChE conjugates

The covalent immobilization of *Dm.* AChE on the carboxyl-covered QDs was performed through the coupling reaction of *N*-ethyl-*N*′-(3-dimethylaminopropyl) carbodiimide and *N*-hydroxysulfosuccinimide; 1,000.0 μL of each EDC (2.0 mg/mL) and sulfo-NHS (6.0 mg/mL) stock

solutions in phosphate buffer (KH_2PO_4 25.0 mM, pH 7.0) were added to a solution of QDs in phosphate buffer and the reaction mixture was stirred for 2 h at room temperature. Subsequently, 1,000.0 μL of *Dm.* AChE (2.0 U/mL) solution were added and after other 2 h of vortexing at room temperature, the mixture was placed at 4 °C overnight. As a follow-up, the QD/AChE conjugates were separated from the unbound enzyme by three rounds of centrifugation/washing (4,000 rpm, 15 min) with phosphate buffer (25.0 mM, pH 7.0) on a Millipore Amicon Ultra filter with a molecular weight cutoff, MWCO of 100,000 (purchased from Malva S.A.). After the first centrifugation, the lower phase was checked for *Dm.* AChE activity. Only negligible *Dm.* AChE activity was detected, proving that almost all enzyme was successfully conjugated to the CdSe/ZnS quantum dots.

Preparation of poly-L-lysine templated QD/AChE/PLL/silica nanocomposites

For the bio-inspired silicification reaction, a 1.0 mM PLL solution was added to the QD/AChE conjugates and after 30 min of mixing in a vortex at room temperature, the mixture was stored at 4 °C overnight. Then, a freshly prepared solution of silicic acid (stock solution prepared by TMOS hydrolysis at a concentration of 1.0 M with 1.0 mM HCl solution) and nanopure H_2O were added, and after being mixed in a vortex for 3–4 h at room temperature, the product was subjected to four rounds of centrifugation/washing with 25.0 mM phosphate buffer, pH 7.0, at 4,000 rpm. The washed silica biomimetic composites were stored at 4 °C in phosphate buffer for further use. Poly-L-lysine templated silica and AChE/PLL/silica nanocomposites were prepared according to our recently published method [40, 41] by adding the corresponding amounts of phosphate buffer (for poly-L-lysine templated silica) and *Dm.* AChE (for AChE/PLL/silica nanocomposites), respectively. The isoelectric point of *Dm.* AChE is 5.0 [40], thus, at the pH where all experiments are performed (pH 7.0), the enzyme is negatively charged. The electrostatic interaction between the negatively charged enzyme and the positively charged poly-L-lysine template promotes the entrapment of the enzyme during biosilicification.

In all cases, *Dm.* AChE activity was measured photometrically at 412 nm according to Ellman's method [44], in 25.0 mM phosphate buffer, pH=7.0 at room temperature.

The schematic diagram for the development of the QD/AChE/PLL/silica nanocomposites is presented in Fig. 1.

Characterization of QD/AChE/PLL/silica nanocomposites

High-resolution transmission electron microscopy (HR-TEM) images of QD/AChE/PLL/silica nanocomposites were obtained using a JEOL JEM-2100 Electron Microscope, operating at 200 kV. The samples for HR-TEM analysis were prepared by evaporation of droplets placed on Formvar/Carbon-coated TEM grids (Analytical Instruments S.A.). The solvent was allowed to evaporate under atmospheric conditions. The ATR-FT-IR spectra were recorded on a Thermo-Electron Nicolet 6700 FT-IR optical spectrometer with a DTGS KBr detector at a resolution of 2 cm^{-1}. Optical measurements were performed at room temperature with a UV–vis spectrophotometer (UNICAM 8625). Quartz Suprasil optical cuvettes for fluorescence measurements (light path of 10 mm) were obtained from Hellma. Fluorescence spectra have been recorded on an Aminco-Bowman series 2 luminescence spectrometer equipped with a continuous high power xenon lamp. All samples were analyzed at room temperature with excitation and emission slits set at 4 nm band-pass and a scan rate of 3 nm/s.

Assay conditions and photoluminescence measuring procedure

To study the pH effect on the photoluminescence intensity of the MUA-covered QDs, a series of solutions with different pH (4.84, 5.22, 5.45, 5.79, 6.57, 6.82, 7.08, 7.54, 8.30, and 8.93) were prepared by adding various amounts of KOH (1.0 M) to a 2.0 mL MES-buffered solution (1.0 mM, pH 4.55). For the assay, 10.0 μL of MUA-covered QDs were mixed with 990.0 μL of the pH solution and left to incubate for 20 min before recording the photoluminescence intensities. All experiments were repeated in triplicate.

To follow the photoluminescence changes that appear upon development of the enzymatic reaction, all measurements were performed by adding the substrate to a cuvette containing the solution of QD/AChE/PLL/silica nanocomposites and recording the photoluminescence intensity of the QDs for more than 20 min. The pores of the silica matrix allow the substrate to enter in its internal nanoenvironment where the enzymatic reaction takes place.

Results and discussions

In this study, a photoluminescence detection system for the enzymatic reaction of the *Dm.* AChE based on highly photoluminescent quantum dots was developed by covalently immobilizing the enzyme on the surface of CdSe/ZnS QDs and further entrapment into bio-inspired silica. The catalytic reaction of AChE is followed by the photoluminescence changes of the CdSe/ZnS core/shell quantum dots.

In order to verify the successful formation of bio-inspired silica shell around the quantum dots and to

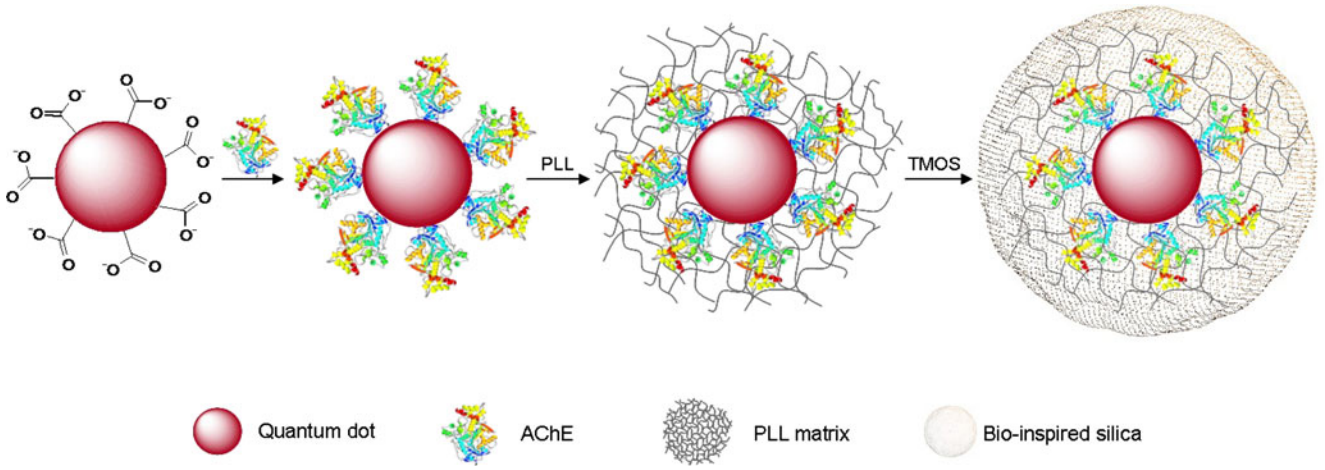

Fig. 1 Schematic representation of the development of the QD/AChE/PLL/silica nanocomposites

determine the morphology of the formed QD/AChE/PLL/silica nanocomposites, fluorescence spectroscopy and HR-TEM were employed. Figure 2 presents the photoluminescence spectra of CdSe/ZnS QDs prior to any modification (solid line) and of the QD/AChE/PLL/silica nanocomposites (dashed line). It can be observed that the photoluminescence spectrum of the QDs entrapped into the bio-inspired silica does not show any significant shift in comparison to the bare QDs, which proves that the encapsulation process does not influence the QDs photoluminescence. The inset in Fig. 2 represents the HR-TEM image of the mercaptoundecanoic acid-capped CdSe/ZnS QDs after entrapment into the bio-inspired silica matrix. As it can be seen from this image, the silicification process produced a uniform structure which completely encapsulates and protects the QDs within the silica matrix without

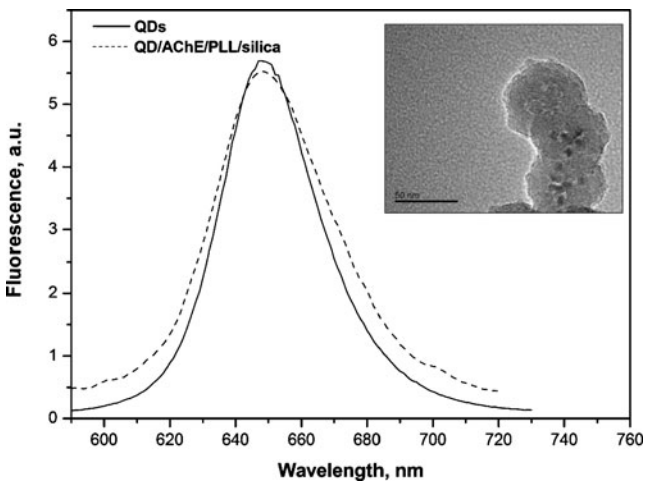

Fig. 2 Photoluminescence spectra of CdSe/ZnS QDs prior to modifications (*solid line*) and of QD/AChE/PLL/silica nanocomposites (*dashed line*). The inset represents the HR-TEM image of the mercaptoundecanoic acid-capped CdSe/ZnS after entrapment into the bio-inspired silica matrix (*bar* 50 nm)

producing the aggregation of the QDs. The formed poly-L-lysine templated QD/AChE/silica nanocomposites are mainly spherical, with a size distribution from 45 to 85 nm in diameter (main population with an average diameter of 63 nm) while an average of six QDs are entrapped in each nanocomposite.

The efficient entrapment of QD/AChE conjugates within the silica architecture was also examined by ATR-FT-IR spectroscopy. The spectrum of poly-L-lysine templated QD/AChE/silica nanocomposites was recorded and subsequently compared to those of poly-L-lysine templated silica nanocomposites and of poly-L-lysine templated AChE/silica nanocomposites. The ATR-FT-IR spectra presents the characteristic peaks of the amide I and amide II bands in the region 1,400–1,700 cm^{-1} as well as the peaks of silica, denoted A, B, and C, that appear in the region 760–1,300 cm^{-1} (Fig. 3a). Amide I and II vibrations of the polypeptide backbone are very sensitive to changes that might appear in the secondary conformations [45, 46] and thus they are monitored closely. The shape of the amide I band (1,620–1,680 cm^{-1}) can provide information on the type and amount of secondary structure [47]. As can be seen from Fig. 3b, the amide I peak of all poly-L-lysine templated silica nanocomposites (PLL/silica, AChE/PLL/silica and QD/AChE/PLL/silica respectively) is shifted in comparison to the one of the solid poly-L-lysine and that of the *Dm.* AChE. Among these, the poly-L-lysine templated QD/AChE/silica nanocomposites display the highest amide I shift toward lower wavenumbers confirming the interaction of poly-L-lysine and protein residues with the silica network. These observed shifts of the amide I peak are due to electrostatic and/or hydrophobic interactions of poly-L-lysine and/or *Dm.* AChE with the silica matrix [48, 49].

Si–O–Si asymmetrical and symmetrical stretching modes, respectively, give rise to silica peaks A and C, while peak B it is attributed to Si–O stretching mode either

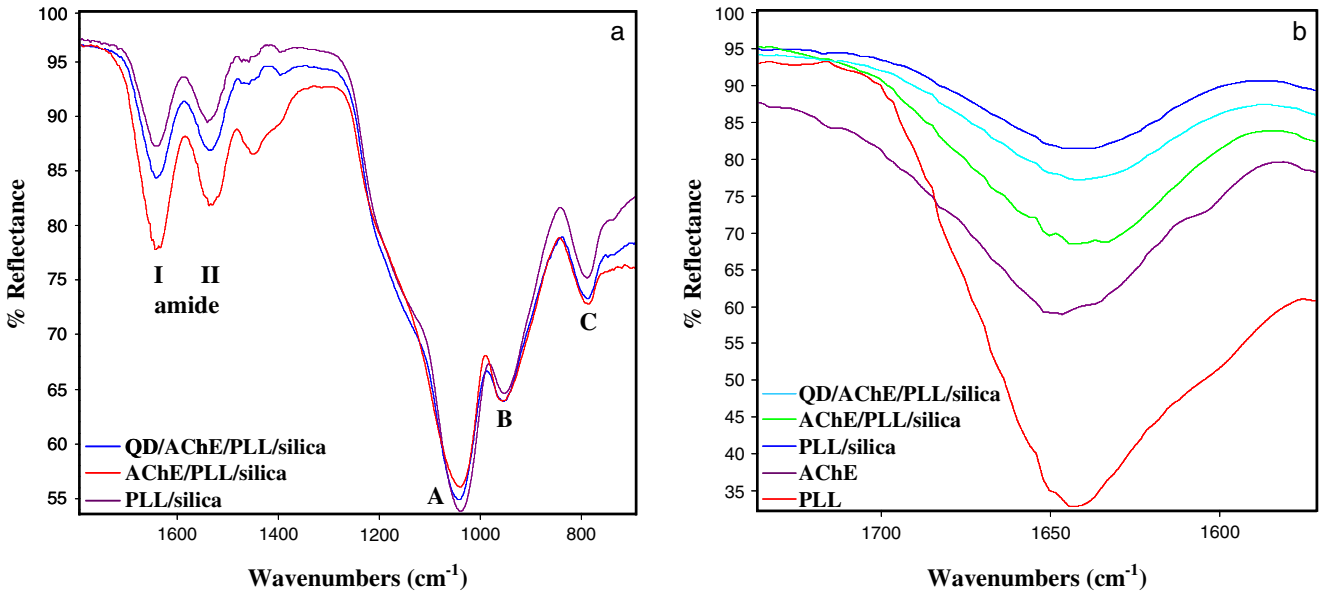

Fig. 3 ATR-FT-IR spectra of bio-inspired silica nanocomposites: PLL/silica, AChE/PLL/silica and QD/AChE/PLL/silica (**a**) and amide I band of *Dm.* AChE, PLL and bio-inspired silica nanocomposites (PLL/silica, AChE/PLL/silica and QD/AChE/PLL/silica) (**b**)

as siloxane bridge (Si–O^-) or as silanol group (Si–OH) [50–53]. The maximum of the main silica peak (A), for all poly-L-lysine templated silica nanocomposites, appears in the region 1,039–1,043 cm^{-1}, as compared to the corresponding silica peak that appears in the region 1,070–1,100 cm^{-1} of other sol–gel silica [54, 55]. This shift can be attributed to the entrapment of AChE and of the QDs/AChE within the silica matrix, which affects the bond strength of neighboring Si–O–Si groups. From these data, it is concluded that the enzyme is indeed entrapped within the silica matrix, and that it also exists a close interaction of the surface functional groups of the protein with the QD/silica nanocomposite sites.

Acetylcholinesterase hydrolyses the substrate acetylcholine producing choline and acetic acid as it is shown in the following scheme:

$$\text{Acetylcholine} + H_2O \xrightarrow{\text{AChE}} \text{Choline} + \text{Acetic Acid}$$

The optimum catalytic activity of *Dm.* AChE is achieved in aqueous solutions of neutral pH. The surface of the CdSe/ZnS core/shell quantum dots used is composed of mercaptoundecanoic acid chains which are pH sensitive. In order to determine the working pH range of the quantum dots, their photoluminescence was recorded in buffered solutions of different pH. As can be seen from Fig. 4, there is a linear relationship between the pH value of the solution and the photoluminescence signal of the QDs for a pH range between 5.45 and 7.54. It is expected that the enzymatic reaction will alter the pH of the immediate surroundings of the QDs because of the acetic acid production. In order to ensure the highest possible photoluminescence sensitivity upon enzymatic reaction, pH 7.0 was chosen, which is the optimum pH for both the enzymatic reaction of acetylcholinesterase and the mercaptoundecanoic acid-capped QDs.

In the next step, the response of the QD/AChE/PLL/silica nanocomposites to the substrate acetylcholine chloride was evaluated. The substrate was added to the silica nanocomposites and the photoluminescence signal of the QDs was monitored over time. Upon addition of substrate, the acetic acid produced by the enzymatic reaction lowers the pH of the surrounding environment of the QDs which quenches their photoluminescence, and, as a result, the

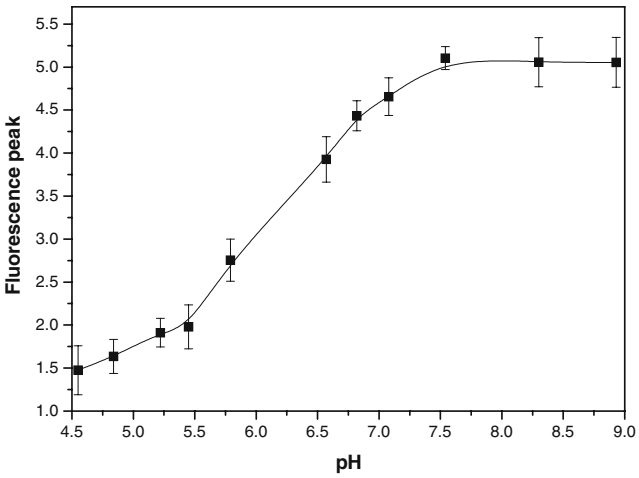

Fig. 4 The changes that appear in the photoluminescence signal of the CdSe/ZnS core/shell quantum dots (excitation 470 nm) recorded at different pH values

higher the substrate concentration is, the higher the quantity of acetic acid to be produced and so the larger the decrease in the observed photoluminescence.

Figure 5 shows the response of the QDs based system to a large scale of substrate concentrations and a linear relationship between the concentration of the substrate and the enzyme activity has been found in the range of 100–1,000 μM (detailed in the inset) with a limit of detection of 1 μM.

Subsequently, the stabilizing effect that the biomimetically synthesized silica has on the QD/AChE complex was evaluated, as compared to the free complex in solution. The stability effect was examined by measuring the response to the substrate over time. As it can be observed from Fig. 6, the QD/AChE/PLL/silica biosensor presents a remaining activity of 100% after 5 days. The following days, the activity slowly decreases, but still remains at a level of 65% after 45 days of measurements. In comparison, the activity of the QD/AChE composites not encapsulated into the biomimetically synthesized silica showed a considerable decrease of their activity to only 50% after 20 days. It is thus evident that the biomimetically synthesized silica provides a stable environment within which the relatively unstable *Dm.* AChE is stabilized.

It is important to note that even the very small QDs concentration used (1.96×10^{-6} mol/L) and the very small amount of enzyme incorporated into the biosensors (only 2 U/mL in the initial solution) are sufficient to obtain a stable biosensor system with a reliable photoluminescence response. This suggests that using the system composed of the QD/AChE conjugates entrapped in the bio-inspired silica, AChE inhibitors could also be detected with good sensitivity.

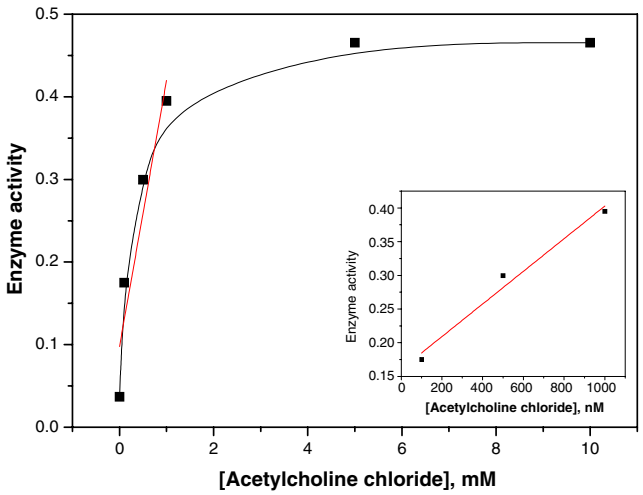

Fig. 5 Calibration curve of the QD/AChE/PLL/silica biosensor. The *inset* represents the linear range of response

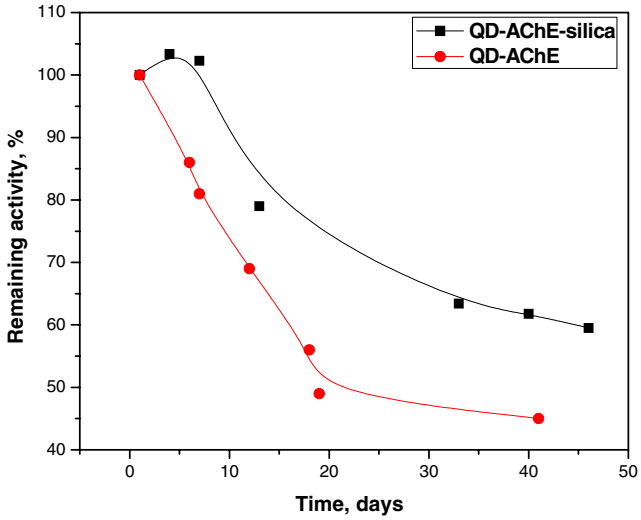

Fig. 6 Stability study of the QD/AChE entraped into the bio-inspired silica nanocomposites compared to the QD/AChE complex free in solution

Conclusions

In this work, we report on a new optical biosensor system based on CdSe/ZnS QDs conjugated to *Dm.* AChE and entrapped into bio-inspired silica matrix based on poly-L-lysine. The pores of the bio-inspired silica nanocomposites allow for the transport of the substrate to the enzyme, while prevent the proteases from reaching the proteins. The bio-inspired silica nanocomposites provide protection of the sensitive QDs from the external environment and prevent the release into the outer environment of toxic atoms that can be desorbed from the surface of the QDs while at the same time they help the enzyme to be stabilized against unfolding or denaturation. The silicification process was investigated by HR-TEM and ATR-FT-IR techniques. It is shown that this process provides nanoporous material with uniform structure which completely encapsulates and protects the QDs within the silica matrix without producing separate aggregates. The response of the QD/AChE/PLL/silica nanocomposites to the AChE substrate acetylcholine chloride was evaluated and a linear relationship between the concentration of the substrate and the enzyme activity has been found in the range of 100–1,000 μM. The bio-inspired nanocomposites have been also tested for their stability over time. It is shown that the activity is retained at a level of 65% after 45 days. In comparison, the activity of the QD/AChE composites not encapsulated into the biomimetically synthesized silica retains only 50% of their initial activity after 20 days.

The entrapment of QD/AChE conjugates into the bio-inspired silica nanocomposites offers an optically active biosensor that proves to be suitable for monitoring low-substrate concentrations

in solution. These QD-based biosensors can provide stable and sensitive nano-biosensor platforms for the detection of the enzymatic activity.

Acknowledgments This work is being supported by the programs NANOMYC (Contract No. 036812) and SANTS (Contract No. 033254) of the European Commission. The authors would like to thank Mrs. Sevasti Papadogiorgaki and Mrs. Alexandra Siakouli from the "Vassilis Galanopoulos" Electron Microscopy Laboratory, for assistance with the transmission electron microscopy.

References

1. Kulzer F, Kummer S, Matzke R, Bräuchle C, Basche T (1997) Nature 387:688–691
2. Satsoura D, Leber B, Andrews DW, Fradin C (2007) Chemphyschem 8:834–848
3. Dickson RM, Cubitt AB, Tsien RY, Moerner WE (1997) Nature 388:355–358
4. Yu WW, Chang E, Drezek R, Colvin VL (2006) Biochem Biophys Res Commun 348
5. Neeleshwar S, Chen CL, Tsai CB, Chen YY, Chen CC, Shyu SG, Seehra MS (2005) Phys Rev B 71:201307(R)
6. Danek M, Jensen KF, Murray CB, Bawendi MG (1996) Chem Mater 8(1):173–180
7. Medintz IL, Uyeda HT, Goldman ER, Mattoussi H (2005) Nat Mater 4:435–446
8. Chan WCW, Nie S (1998) Science 281:2016–2018
9. Willard DM, Carillo LL, Jung J, Van Orden A (2001) Nano Lett 1 (9):469–474, 781–786
10. Patolski F, Gill R, Weizmann Y, Mokari T, Banin U, Willner I (2003) J Am Chem Soc 125:13918–13919
11. Clapp AR, Medintz IL, Mauro JM, Fisher BR, Bawendi MG, Mattoussi H (2004) J Am Chem Soc 126:301–310
12. Hering VR, Gibson G, Schumacher RI, Faljoni-Alario A, Politi MJ (2007) Bioconjug Chem 18:1705–1708
13. Liu YS, Sun Y, Vernier PT, Liang CH, Chong SYC, Gundersen MA (2007) J Phys Chem C 111:2872–2878
14. Huang CP, Li YK, Chen TM (2007) Biosens Bioelectron 22:1835–1838
15. Huang CP, Liu SW, Chen TM, Li YK (2008) Sens Actuators B 130:338–342
16. Du D, Chen S, Song D, Li H, Chen X (2008) Biosens Bioelectron 24:475–479
17. Tang L, Zhu Y, Yang X, Sun J, Li C (2008) Biosens Bioelectron 24:319–323
18. Zhelev Z, Bakalova R, Ohba H, Jose R, Imai Y, Baba Y (2006) Anal Chem 78(1):321–330
19. Kaul Z, Yaguchi T, Kaul SC, Hirano T, Wadhwa R, Taira K (2003) Cell Res 13:503–507
20. Rosenthal SJ, Tomlinson I, Adkins EM, Schroeter S, Adams S, Swafford L, McBride J, Wang Y, DeFelice LJ, Blakely RD (2002) J Am Chem Soc 124:4586–4594
21. Derfus AM, Chen WCW, Bhatia SN (2004) Nano Lett 4:11–18
22. Cho SJ, Maysinger D, Jain M, Röder B, Hackbarth S, Winnik FM (2007) Langmuir 23:1974–1980
23. Graf C, Dembski S, Kruger T, Gbureck U, Ewald A, Bock A, Ruhl E (2008) Small 4(9):1516–1526
24. Kirchner C, Liedl T, Kudera S, Pellegrino T, Javier AM, Gaub HE, Stolzle S, Fertig N, Parak WJ (2005) Nano Lett 5:331–338
25. Daou TJ, Li L, Reiss P, Josserand V, Texier I (2009) Langmuir 25:3040–3044
26. Correa-Duarte MA, Giersig M, Liz-Marzan LM (1998) Chem Phys Lett 286:497–501
27. Rogach AL, Nagesha D, Ostrander JW, Giersig M, Kotov NA (2000) Chem Mater 12:2676–2685
28. Yang Y, Jing L, Yu X, Yan D, Gao M (2007) Chem Mater 19:4123–4128
29. Chang SY, Liu L, Asher SA (1994) J Am Chem Soc 116:6739–6744
30. Selvan ST, Tan TT, Ying JY (2005) Adv Mater 17:1620–1625
31. Darbandi M, Thomann R, Nann T (2005) Chem Mater 17:5720–5725
32. Shukoor MI, Natalio F, Therese HA, Tahir MN, Ksenofontov V, Panthöfer M, Eberhardt M, Theato P, Schröder HC, Müller WEG, Tremel W (2008) Chem Mater 20:3567–3573
33. Leng B, Chen X, Shao Z, Ming W (2008) Small 4(6):755–758
34. Zhang Q, Zhang L, Liu B, Lu X, Li J (2007) Biosens Bioelectron 23:695–700
35. Wolcott A, Gerion D, Visconte M, Sun J, Schwartzberg A, Chen S, Zhang JZ (2006) J Phys Chem B 110(11):5779–5789
36. Avnir D, Braun S, Lev O, Ottolenghi M (1994) Chem Mater 6:1605–1614
37. Lei C, Shin Y, Liu J, Ackerman EJ (2002) J Am Chem Soc 124:11242–11243
38. Fan J, Lei J, Wang L, Yu C, Tu B, Zhao D (2003) Chem Commun 2140–2141
39. Naik RR, Tomczak MM, Luckarift HR, Spain JC, Stone MO (2004) Chem Commun 1684–1685
40. Vamvakaki V, Hatzimarinaki M, Chaniotakis N (2008) Anal Chem 80:5970–5975
41. Hatzimarinaki M, Vamvakaki V, Chaniotakis N (2009) J Mater Chem 19:1–7
42. Patwardhan SV, Mukherjee N, Steinitz-Kannan M, Clarson SJ (2003) Chem Commun 10:1122–1123
43. Dembski S, Graf C, Krüger T, Gbureck U, Ewald A, Bock A, Rühl E (2008) Small 4(9):1516–1526
44. Ellman GL, Courtney KD, Andres V Jr, Featherstone RM (1961) Biochem Pharmacol 7:88–95
45. Krimm S, Bandekar J (1986) Adv Protein Chem 38:181–364
46. Bandekar J (1992) Biochim Biophys Acta 1120:123–143
47. Barth A, Zscherp C (2002) Q Rev Biophys 35:369–430
48. Sotiropoulou S, Chaniotakis NA (2005) Biomaterials 26:6771–6779
49. Wu S, Ju H, Liu Y (2007) Adv Funct Mater 17:585–592
50. Almeida RM, Guiton TA, Pantano CG (1990) J Non-Cryst Solids 121:193–197
51. Perry CC, Li X, Waters DN (1991) Spectrochim Acta 47A:1487–1494
52. Innocenzi P (2003) J Non-Cryst Solids 316:309–319
53. Fidalgo A, Cirimanna R, Ilharco LM, Pagliaro M (2005) Chem Mater 17:6686–6694
54. Bertoluzza A, Fagnano C, Morelli MA, Gottardi V, Guglielmi M (1982) J Non-Cryst Solids 48:117–128
55. Martinez JR, Ruiz F, Vorobiev YV, Perez-Robles F, Gonzalez-Hernandez J (1998) J Chem Phys 109:7511–7514